Green Chemistry

PAPER

View Article Online
View Journal | View Issue

Cite this: *Green Chem.*, 2024, **26**, 10486

Selective hydrogenation of guaiacol to 2-methoxycyclohexanone over supported Pd catalysts†

Yota Taniwaki,[a] Yoshinao Nakagawa, *[a,b] Mizuho Yabushita [a,b] and Keiichi Tomishige *[a,b,c]

Received 1st August 2024,
Accepted 6th September 2024

DOI: 10.1039/d4gc03793f

rsc.li/greenchem

Selective hydrogenation of guaiacol to 2-methoxycyclohexanone was investigated with various Pd catalysts. This reaction is much more difficult than the hydrogenation of phenol to cyclohexanone, namely in terms of the low reactivity of guaiacol and the reduced selectivity of 2-methoxycyclohexanone due to the demethoxylation reaction. Pd/TiO_2 catalysts were found to be superior to other supported Pd catalysts in terms of activity and selectivity to 2-methoxycyclohexanone. The Pd dispersion did not affect the selectivity of Pd/TiO_2 catalysts. Meanwhile, the increase of Pd dispersion decreased the turnover frequency, and the optimum Pd dispersion was about 25%. The presence of residual chloride ions had a negative effect on the selectivity to 2-methoxycyclohexanone. The optimal Pd/TiO_2 catalyst gave 65% yield of 2-methoxycyclohexanone. The catalyst was reusable after washing with toluene solvent to extract residual organic species from the catalyst surface. The catalyst was capable of hydrogenating various phenolic compounds, namely methoxyphenols, into the corresponding cyclohexanone derivatives.

1. Introduction

Amid concerns over the depletion of petroleum, there is growing interest in producing chemicals from biomass resources.[1–4] Lignocellulosic biomass mainly consisting of cellulose, hemicellulose, and lignin is a promising renewable resource due to its abundance. Fast pyrolysis of lignocellulosic biomass or lignin yields liquid compounds (bio-oil) that can be used as both fuel and chemical feedstock.[5–11] However, bio-oil contains a larger number of oxygen atoms and/or double bonds than petroleum. To this end, it is necessary to decrease the O/C ratio and increase the H/C ratio. Moreover, bio-oil is rich in lignin-derived phenolic derivatives and has great potential as a raw material for aromatic compounds and their derivatives. Guaiacol, a simple aromatic compound with a C6 carbon backbone possessing both hydroxy and methoxy groups, shares structural similarities with lignin and many lignin-derived compounds. In addition, the pyrolysis of lignin under appropriate conditions offers bio-oil in which guaiacol is a major component.[12] In this respect, the conversion of guaiacol into valuable chemical products such as benzene, phenol, and cyclohexanol has garnered considerable attention.[13–25]

Adipic acid is one of the most important C6 monomers that serves as a raw material for synthetic polymers and has been a target product of guaiacol conversion. Adipic acid is currently synthesized from petroleum-derived benzene by hydrogenation to cyclohexane, oxidation to K/A-oil, which is a mixture of cyclohexanone and cyclohexanol, and further oxidation with nitric acid.[26,27] Although the environmentally-benign oxidant O_2 is an attractive oxidant, the oxidation of K/A-oil with O_2 is less selective than that with nitric acid and is not used in industrial processes. The production of adipic acid from guaiacol is thus a promising approach for synthesizing renewable adipic acid.[26,28,29]

One approach is the synthesis of K/A-oil by hydrodeoxygenation of guaiacol. However, this route requires a large amount of hydrogen (min 3 eq.) (eqn (1)), and nitric acid oxidation is still necessary. Furthermore, there have been no reports on the direct synthesis of cyclohexanone and methanol expressed as eqn (1). The primary mono-oxygenate product is phenol or cyclohexanol. Hydrogenation of phenol to cyclohexanone is possible, but the process becomes more complex. Cyclohexanol can be used as a substrate for the nitric acid oxidation to adipic acid, but the synthesis of cyclohexanol from guaiacol consumes a larger amount of hydrogen than eqn (1).

[a]*Department of Applied Chemistry, School of Engineering, Tohoku University, 6-6-07 Aoba, Aramaki, Aoba-ku, Sendai, Miyagi 980-8579, Japan. E-mail: yoshinao@erec.che.tohoku.ac.jp, tomishige@tohoku.ac.jp*
[b]*Research Center for Rare Metal and Green Innovation, Tohoku University, 468-1 Aoba, Aramaki, Aoba-ku, Sendai, Miyagi, 980-0845, Japan*
[c]*Advanced Institute for Materials Research (WPI-AIMR), Tohoku University, 2-1-1 Katahira, Aoba-ku, Sendai, Miyagi, 980-8577, Japan*
† Electronic supplementary information (ESI) available. See DOI: https://doi.org/10.1039/d4gc03793f

In addition, most reported systems decompose the methoxy group in guaiacol to methane, which further increases hydrogen consumption.

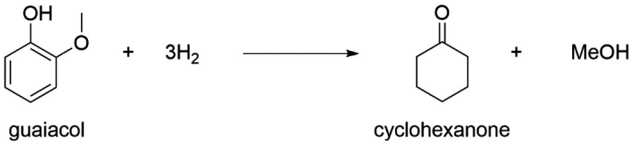

(1)

Recently, our group reported that adipic acid can be synthesized by the oxidative cleavage of 2-methoxycyclohexanone (2-MCO), a partial hydrogenation product of guaiacol, with a heteropoly acid catalyst and O_2 (eqn (2)).[30] The methoxy group can be recovered by methanol. Ideally, the route of adipic acid synthesis *via* 2-MCO consumes less hydrogen (2 eq., consumed in guaiacol to 2-MCO) than the route *via* monooxygenates (3 eq. or more) and can also avoid the nitric acid oxidation step.

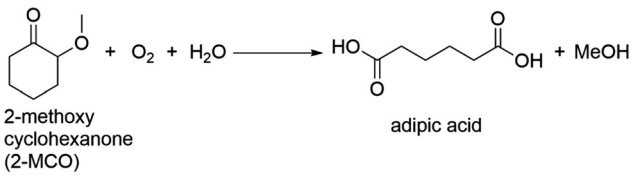

(2)

To establish the production route of adipic acid from guaiacol *via* 2-MCO, selective partial hydrogenation of guaiacol to 2-MCO is necessary (eqn (3)). However, few studies have examined this reaction, and the maximum reported yield with H_2 as a reductant was only 37%.[31] On the other hand, the selective partial hydrogenation of phenol to cyclohexanone, which is a closely related reaction to the current target reaction, has been intensively investigated, and excellent yields have been reported in many studies.[32,33] For the hydrogenation of phenol to cyclohexanone, catalysts with platinum group metals, especially Pd, have been mainly used (Table S1†).[34–46] Pd is known to have excellent hydrogen activation ability and high activity in the hydrogenation of C=C bonds, while the activity of Pd in C=O hydrogenation is low; these features make Pd a good catalyst for the hydrogenation of phenol to cyclohexanone. The effect of supports has been intensively investigated, and base sites and/or Lewis acid sites have been proposed to have a positive effect on the selectivity to cyclohexanone.[47–51] Some studies investigated the selective hydrogenation of phenolic compounds to the corresponding cyclohexanone derivatives. Alkylphenols such as *o*-cresol (2-methylphenol) are typical substrates used in such studies, and excellent yields have also been reported.[31,36,41,44,52–56] Meanwhile, reports on the selective hydrogenation of methoxyphenols to target ketones have been limited, and the performance of reported catalysts was lower than those of other phenolic compounds. Most of the studies tested only 4-methoxyphenol as the substrate among methoxyphenols, despite the fact that guaiacol is a more abundant phenolic compound than methoxyphenol. Even in the studies that investigated guaiacol hydrogenation, the performance of catalysts in the guaiacol hydrogenation was always much lower than those in the hydrogenation of 4-methoxyphenol, *o*-cresol, and catechol. The most typical case is the Pd/HAP (HAP = hydroxyapatite) catalyst which gave the highest yield of 2-MCO. Cyclohexanone, 4-methoxycyclohexanone, and 2-hydroxycyclohexanone were obtained in quantitative yields from phenol, 4-methoxyphenol, and catechol at 3 h, 3.5 h, and 8 h, respectively, while 2-MCO was obtained from guaiacol in only 37% yield (98% selectivity) at 24 h.[31]

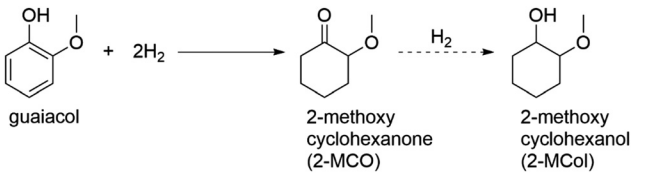

(3)

Syringol (2,6-dimethoxyphenol; possessing two methoxy groups at both *o*-positions of phenol) is another model compound having typical substructures of lignin. The reports on the hydrogenation of syringol to 2,6-dimethoxycyclohexanone are few, and there have been no reports with considerable yield. Partial hydrogenation of these *o*-methoxyphenols to *o*-methoxycyclohexanones is quite challenging, and there have been no reports focusing on this reaction. In this study, therefore, we investigated the partial hydrogenation of guaiacol to 2-MCO over various Pd catalysts because of their good ability for hydrogen activation and low activity for the C=O hydrogenation of Pd species, as alluded to above. The relationship between Pd dispersion and catalytic performance was confirmed, and good yield (65%) was obtained with the optimized Pd/TiO_2 catalyst.

2. Experimental

2.1. Catalyst preparation

All the reagents were commercially available (Table S2†). Pd catalysts were prepared by the typical impregnation method. The Pd precursor was $Pd(OAc)_2$ unless otherwise noted, and the typical Pd loading amount was 3 wt%. The properties of supports are summarized in Table S3.† First, an acetone solution of the Pd precursor ($Pd(OAc)_2$, $Pd(acac)_2$) or an aqueous solution ($PdCl_2$, $Pd(NO_3)_2$, $Pd(NH_3)_4Cl_2$) was added to the support in a beaker until the surface of the support was saturated, and the mixture was stirred well with a glass bar. The beaker containing the wet sample was then placed on a heating plate, and the mixture was dried at 343 K (in the case using either acetone solution or 373 K (aqueous solution)). This process was repeated until the entire precursor solution was consumed. The solids were further dried in a drying oven at 383 K overnight. The dried catalysts except those using carbon-based supports (AC (activated carbon) and CB (carbon black)) were calcined in air at 573 K for 3 h at a heating rate of 10 K min^{-1}. Pd/AC and Pd/CB were directly reduced at 573 K

for 1 h under a H_2 flow (30 mL min^{-1}) at a heating rate of 10 K min^{-1} instead of calcination.

2.2. Activity test and product analysis

The activity tests were carried out in a stainless steel autoclave (190 mL) equipped with a glass inner vessel. The substrate, solvent (typically water), and catalyst were put into the autoclave together with a spinner. After the purge process of the autoclave with H_2 three times, the autoclave was filled with 1 MPa H_2 (at r.t.) and then heated to the designated temperature. The reaction time was counted from the time when the inner temperature monitored with a thermocouple reached 5 K below the target one. After an appropriate reaction time, the reactor was rapidly cooled in a cold-water bath. The gas phase was collected in a gas bag. The liquid phase was collected with 1,4-dioxane, and the catalyst powder was removed by filtration with a syringe filter.

The quantification of products in the gas phase was carried out with a gas chromatograph (GC; Shimadzu GC-2014) equipped with a Porapak N packed column, a methanator, and a flame-ionization detector (FID). The products in the liquid phase were analyzed with a GC (Shimadzu GC-2025) equipped with a TC-WAX column (diameter 0.25 mm, length 30 m) and a FID. The conversion, yield, selectivity, carbon balance, and conversion rate were calculated using the following equations:

$$\text{Conversion}(\%) = \frac{\text{mole of substrate consumed}}{\text{mole of input substrate}} \times 100 \quad (4)$$

$$\text{Yield}(\%) = \frac{\text{C-based mole of product}}{\text{C-based mole of input substrate}} \times 100 \quad (5)$$

$$\text{Selectivity}(\%) = \frac{\text{C-based mole of product}}{\text{sum of C-based mole of products}} \times 100 \quad (6)$$

$$\text{Carbon balance}(\%) = \frac{\text{sum of C-based mole of products} + \text{C-based mole of residual substrate}}{\text{C-based mole of input substrate}} \times 100 \quad (7)$$

$$\text{Guaiacol conversion rate } (\text{mmol } g_{Pd}{}^{-1}\ h^{-1}) = \frac{\text{sum of C-based mole of products}/7}{\text{mass of input Pd(g)} \times \text{reaction time(h)}} \times 1000 \quad (8)$$

$$\text{TOF}(h^{-1}) = \frac{\text{sum of C-based mole of products}/7}{\text{mole of input Pd} \times \text{dispersion} \times \text{reaction time(h)}} \quad (9)$$

The carbon balance values were typically 100 ± 5% as shown in any tables in the ESI.† The selectivity calculated using eqn (6) might involve some overestimation because of the formation of unidentified products (within a few percent considering the carbon balance values).

Catalyst reuse tests were conducted as follows: the reaction was carried out in multiple autoclaves under the same conditions. The used catalysts were collected from each autoclave by filtration and mixed together. The mixed sample was washed with water (30 g) and dried at 383 K overnight. The dried catalyst was calcined at 573 K, if necessary. The total loss of catalyst during the recovery and regeneration processes was less than the amount necessary for one batch, and the next cycle of reaction was carried out with fewer autoclaves by one under the same conditions. For the washing process with toluene, the collected catalyst samples were first washed with water (30 g), followed by washing with toluene (30 g); afterward, the resulting samples were dried at 383 K overnight.

2.3. Characterization

Thermogravimetry-differential thermal analysis (TG-DTA) was carried out with a Rigaku Thermo Plus EVO-2 in an air flow (30 mL min^{-1}). Wavelength dispersive X-ray fluorescence spectroscopy (XRF) was carried out with Bruker S8 Tiger apparatus, and Si in SiO_2 was used as an internal standard. A Rigaku MiniFlex600 diffractometer (Cu Kα radiation) was used to acquire the X-ray diffraction (XRD) patterns of each sample. A catalyst analyzer BELCAT II (MicrotracMRB; equipped with a thermal conductivity detector) was used for CO chemisorption measurement. Prior to each run, the catalyst was reduced under a H_2 flow (50 mL min^{-1}) at 473 K for 30 min; afterward, CO pulses were introduced to the catalyst bed at 323 K. Pd dispersion was calculated as the ratio of the adsorbed CO amount to the total Pd amount. Scanning transmission electron microscopy (STEM) images were taken with a HITACHI HD-2700. For STEM measurement, the catalyst was reduced in water with 1 MPa H_2 at 373 K (*i.e.*, liquid phase reduction), dispersed in ethanol, and dropped on a Cu microgrid. ^{1}H nuclear magnetic resonance (NMR) spectroscopy was carried out with a Bruker AV400 spectrometer (^{1}H 400 MHz), and toluene-d_8 was employed as a deuterated solvent. The methyl group (2.08 ppm) of toluene-d_8 was used to calibrate the chemical shift.

3. Results and discussion

3.1. Optimization of the catalyst

3.1.1. Support effect. As summarized in Table 1, the screening of supports for Pd catalysts in the selective hydrogenation of guaiacol at 373 K was initially conducted. The detailed data including the selectivity to each detected product are shown in Table S4.† For the fair comparison of product selectivity shown by each catalyst, the reactions were also carried out at ~20% level of conversion by controlling the reaction time, and the results are shown in Table S5.† The dispersion of Pd determined by CO adsorption is also listed in Table 1. The target product, 2-methoxycyclohexanone (2-MCO), was the major product for all the Pd catalysts except for Pd/H-ZSM-5 and Pd/CB. Pd/H-ZSM-5 gave mainly 2-methoxycyclohexanol (2-MCol) which is the over-hydrogenation product, while Pd/CB was almost inactive. 2-MCol was also produced to some extent for all the active Pd catalysts. Cyclohexanone and other demethoxylation products were also detected, and the methoxy group was converted to methanol (carbon yield of C6 : methanol = 6 : 1). Pd/CeO_2, Pd/SiO_2, Pd/TiO_2, and Pd/AC gave relatively high conversion and 2-MCO yield. The high

Table 1 Selective hydrogenation of guaiacol over Pd catalysts with various supports

				Yield [C based] (%)				
				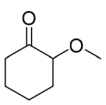	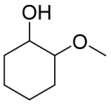	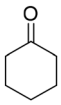		
Entry	Catalyst	D^a (%)	Conv. (%)	2-MCO	2-MCol		Others	Methanol
1	Pd/α-Al_2O_3	13.5	16.2	9.6	0.4	1.3	0.5	0.2
2	Pd/BN	6.5	8.1	3.2	0.8	0.1	0.3	0.0
3	Pd/H-ZSM-5	19.2	23.5	0.3	14.9	3.4	1.3	2.0
4	Pd/CeO_2	57.6	56.4	20.8	13.8	9.0	6.7	2.3
5	Pd/SiO_2	29.4	45.0	33.0	6.7	4.6	2.9	1.0
6	Pd/Nb_2O_5	43.6	13.6	6.0	1.9	0.6	1.0	0.2
7	Pd/TiO_2 (anatase)	24.4	40.6	29.6	5.7	2.0	0.6	0.4
8	Pd/TiO_2 (rutile)	15.3	15.3	7.2	1.6	1.0	1.6	0.2
9	Pd/TiO_2 (P25)	17.4	33.3	24.0	3.3	2.0	1.1	0.4
10	Pd/HAP	21.4	10.4	7.3	0.7	0.4	0.3	0.1
11	Pd/AC	18.2	29.8	18.7	6.1	0.3	0.5	0.1
12	Pd/CB	6.9	4.6	0.1	0.0	0.0	0.0	0.1

Reaction conditions: guaiacol (0.62 g), catalyst (Pd = 3 wt%, 100 mg), water (10 g), 373 K, H_2 (1 MPa at r.t.), 4 h. HAP: hydroxyapatite, AC: activated carbon, CB: carbon black. ^{a} Dispersion(%) $= \left[\frac{\text{amount (mol) of adsorbed CO}}{\text{total amount(mol) of Pd}}\right] \times 100$.

activity can be mostly explained by the higher dispersion of Pd, although there were some exceptions such as Pd/Nb_2O_5 with low activity and high dispersion. Among the three TiO_2 supports, the activity of Pd/TiO_2 catalysts decreased in the order of anatase > P-25 (anatase-rich anatase-rutile mixture) > rutile. Even with consideration of Pd dispersion, anatase pro-

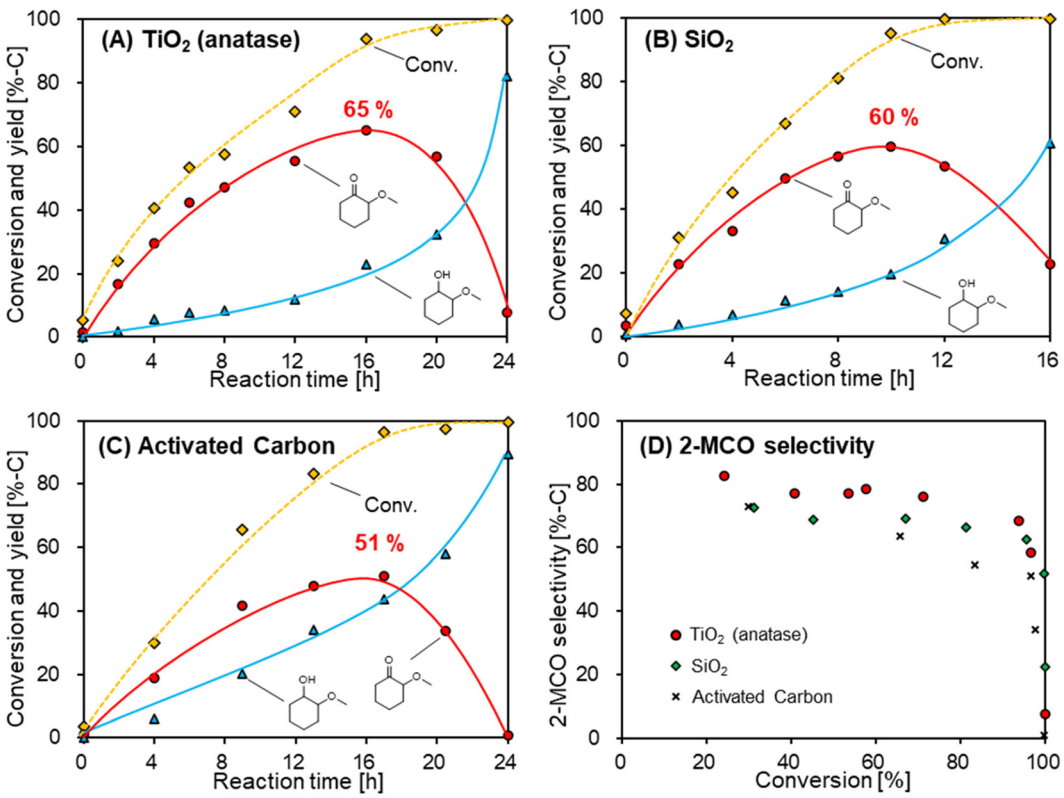

Fig. 1 Time courses of selective hydrogenation of guaiacol over Pd catalysts on various supports. Conditions: guaiacol (0.62 g), catalyst (Pd = 3 wt%, 100 mg), water (10 g), 373 K, H_2 (1 MPa at r.t.). (A): Anatase TiO_2 support, (B) SiO_2 support, (C) activated carbon support, and (D) selectivity of 2-MCO.

vided higher activity than rutile. Furthermore, Pd/TiO_2 (anatase) showed the highest selectivity to 2-MCO when compared at a similar conversion level (Table S5†). The Pd/HAP catalyst, which was reported to exhibit high selectivity to 2-MCO,[31] showed low activity regardless of its comparable Pd dispersion to Pd/TiO_2 (anatase). The selectivity of Pd/HAP to 2-MCO was similarly high to Pd/TiO_2 (anatase), agreeing with the literature. Pd/CeO_2 showed the highest conversion of guaiacol; however, the formation of byproducts such as 2-MCol and cyclohexanone was significantly large. This result is consistent with previous reports where Pd/CeO_2 was reported to be an effective catalyst for the hydrogenolysis of guaiacol to cyclohexanol and cyclohexanone.[57]

Next, the time courses of the hydrogenation of guaiacol were compared among Pd/TiO_2 (anatase), Pd/SiO_2, and Pd/AC (Fig. 1; detailed data: Table S6†). The conversion reached 100% for all the three catalysts with enough reaction time. The yield of 2-MCO increased at the initial stage and then decreased because of the over-hydrogenation of 2-MCO to 2-MCol. The highest yield of 2-MCO (65%-C) was obtained over Pd/TiO_2 (anatase). This yield value significantly surpasses previously reported yields of up to 37%.[31] The lower selectivity of Pd/SiO_2 and Pd/AC than that of Pd/TiO_2 (anatase) was also confirmed by the conversion–selectivity plots (Fig. 1D): the selectivity of Pd/TiO_2 (anatase) was higher than those of Pd/SiO_2 and Pd/AC in the entire conversion range. These results indicate that TiO_2 (anatase) is the best among the supports tested for the Pd-catalyzed guaiacol hydrogenation to 2-MCO. Pd/TiO_2 (anatase) was thus employed in the following study and hereafter denoted as Pd/TiO_2.

3.1.2. Optimization of the composition and preparation method for the Pd/TiO_2 catalyst. For further optimization of Pd/TiO_2, various Pd/TiO_2 catalysts were prepared by changing the Pd precursor, Pd loading amount, and calcination temperature. The performance of the prepared catalysts is summarized as a function of Pd dispersion in Fig. 2, and the details of the catalysts are described in Table S7 and Fig. S1.† For the activity of Pd/TiO_2 catalysts (Fig. 2A), the results exhibited a

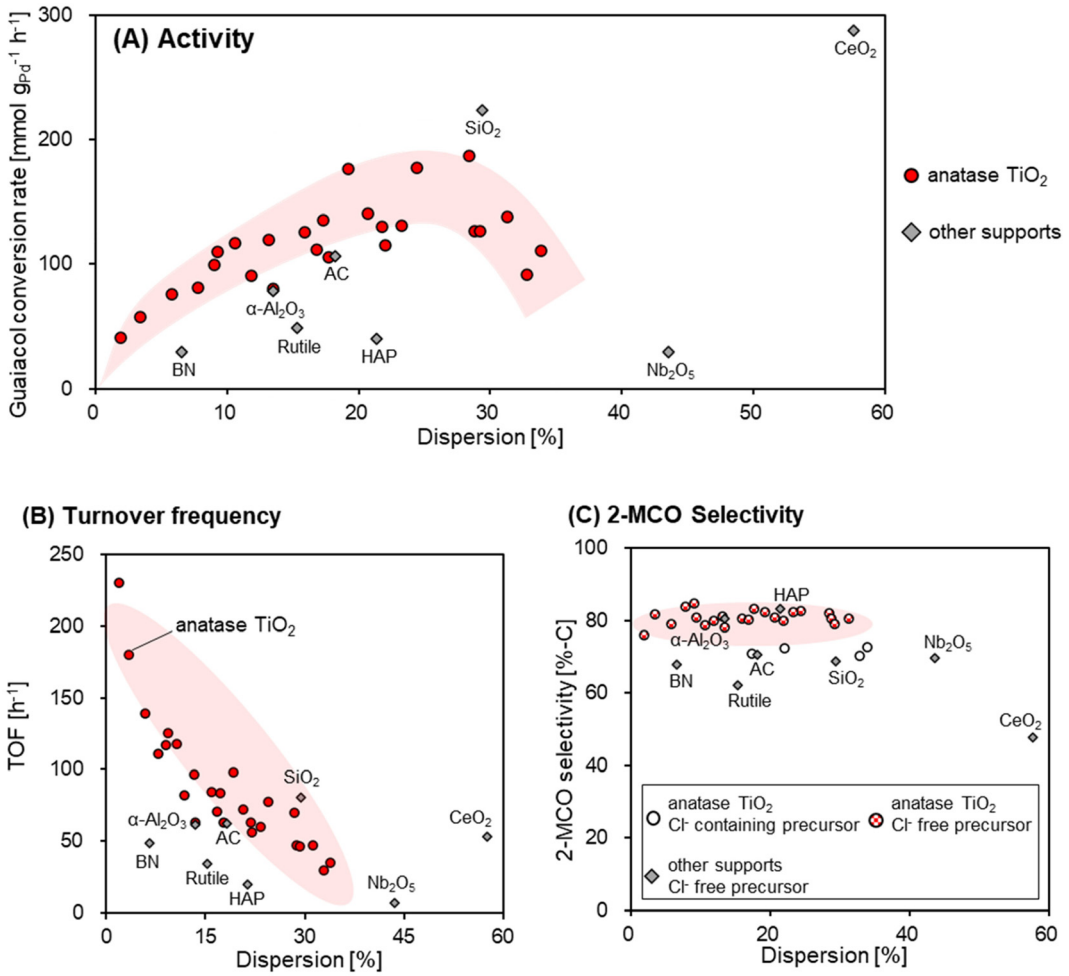

Fig. 2 Correlation between Pd dispersion and the catalytic activity of selective hydrogenation of guaiacol over supported Pd catalysts. (A) Guaiacol conversion rate, (B) turnover frequency, and (C) 2-MCO selectivity. Conditions: guaiacol (0.62 g), catalyst (100 mg), water (10 g), 373 K, H_2 (1 MPa at r.t.). Dispersion (%) $= \left[\frac{\text{amount(mol) of adsorbed CO}}{\text{total amount(mol) of Pd}}\right] \times 100$.

volcano-type correlation; the catalytic activity increased with increasing dispersion up to about 25% and then decreased. Meanwhile, the turnover frequency (TOF) calculated at about 20% level of conversion based on the CO adsorption amount (the number of active sites) (Fig. 2B) decreased upon an increase in Pd dispersion; the TOF decreased from ~200 h^{-1} (<5% Pd dispersion) to <50 h^{-1} (>30% Pd dispersion). A part of the TOF decrease could be due to the change of the adsorption mode of CO from bridge (CO/Pd = 0.5–1) to linear (CO/Pd = 1), but the factor is not more than 2.[58] The results of the other Pd/support catalysts are also plotted in Fig. 2. The activity of Pd/AC and Pd/SiO_2 was in the similar range of Pd/TiO_2 with the same Pd dispersion. The activity of Pd/CeO_2 seems to be greatly higher than that of Pd/TiO_2 owing to the better Pd dispersion, while the TOF value based on the number of surface Pd atoms was not as high as Pd/TiO_2. The other supports showed lower activity compared to the Pd/TiO_2 catalysts.

For the selectivity to 2-MCO at about 20% level of conversion (Fig. 2C), all the Pd/TiO_2 catalysts showed similar selectivity to 2-MCO regardless of the Pd dispersion. Nevertheless, some Pd/TiO_2 catalysts showed slightly lower selectivity, and the common feature was the use of a Cl^--containing precursor. To this end, the effect of residual Cl^- in the reaction system was investigated through control reactions by adding HCl with the Cl^--free catalyst (Fig. 3; detailed data: Table S8†). The addition of HCl to the system with the Pd/TiO_2 catalyst prepared from $Pd(OAc)_2$ slightly increased the activity while decreasing the selectivity to 2-MCO. The increased byproducts were cyclohexanone and 2-hydroxycyclohexanone (hydrolysis product of 2-MCO). The effect of H^+, which was inevitably added to the system due to the use of HCl, was checked by further control experiments using H_2SO_4 as an additive; however, the addition of H_2SO_4 did not affect the activity or selectivity. These results indicated that the presence of Cl^- has negative effects on the selective hydrogenation to 2-MCO. In view of both activity and selectivity, the Pd/TiO_2 catalyst prepared from the Cl^--free precursor with about 25% dispersion was the optimum catalyst; such a catalyst was obtained successfully with 3 wt% loading, $Pd(OAc)_2$ as the precursor, and calcination at 573 K after Pd loading, *i.e.*, the Pd/TiO_2 (anatase) catalyst displayed in Table 1 and Fig. 1.

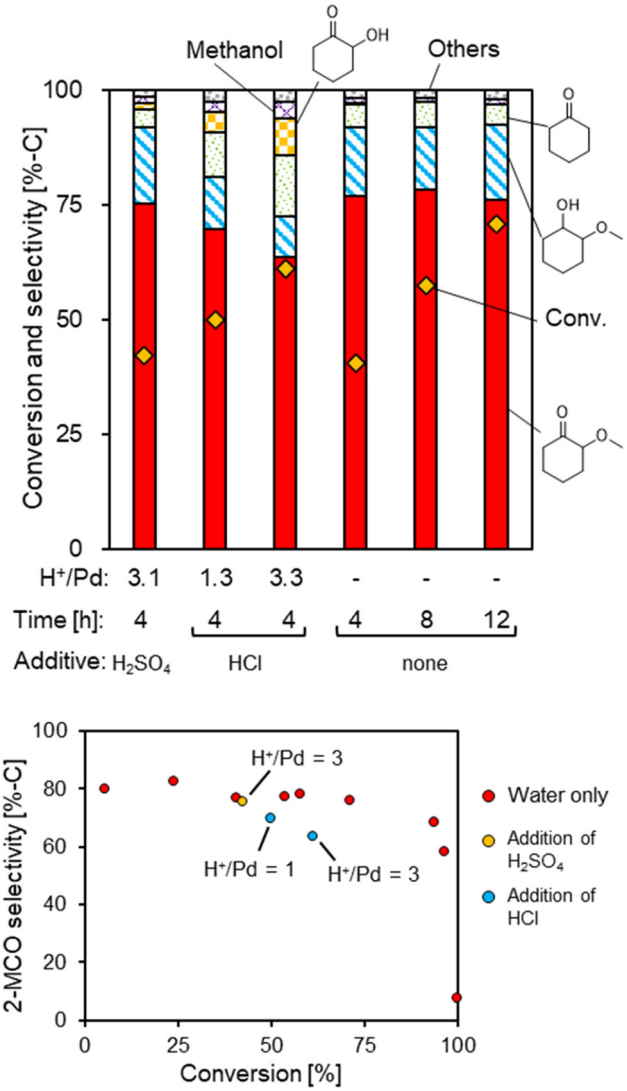

Fig. 3 Effect of chloride ions on the selective hydrogenation of guaiacol over the Pd/TiO_2 catalyst. Conditions: guaiacol (0.62 g), Pd/TiO_2 (Pd = 3 wt%, 100 mg), water (10 g), 373 K, H_2 (1 MPa at r.t.).

3.1.3. Characterization of the optimal catalyst and the possible active structure. The optimized Pd/TiO_2 catalyst was characterized by XRD and STEM analyses (Fig. 4). The XRD pattern displayed the broad peak of fcc Pd(111) overlapping with the peak of anatase TiO_2. In the STEM image, metal nanoparticles with approximately 3 nm size were observed. These results do not contradict the known correlation[59] between the particle size and dispersion elucidated from CO adsorption (24%; Table 1).

Here we discuss the possible active structure in the guaiacol hydrogenation to 2-MCO. The strong negative correlation between the TOF and Pd dispersion of the Pd/TiO_2 catalysts (Fig. 2 and Fig. S1†) suggests that the simple flat surface (terrace sites) of the Pd metal phase is active for this reaction, and the corner and/or edge sites are rather inactive. This structure sensitivity can be explained by the reaction model drawn in Fig. 5 where the aromatic ring of guaiacol is adsorbed in a planar mode onto the terrace site of the Pd metal and the hydrogenation proceeds by the reaction of the adsorbed aromatic ring and hydrogen atoms also adsorbed on the Pd surface.[60,61] In addition, the effect of the TiO_2 support is not positive because the support effect becomes stronger with the decrease of particle size (increase of dispersion). The reaction mechanism will be further discussed in the later section after discussing the solvent effect, kinetics, and substrate scope. For the catalysts with other supports, the activity and selectivity of the Pd-support interface sites can be considered. Some catalysts (Pd/BN, Pd/TiO_2 (rutile), and Pd/HAP) show lower activity than the Pd/TiO_2 catalysts (Fig. 2). The possible explanation is that the Pd-support interface sites have lower activity than the Pd-TiO_2 ones. Moreover, Pd/HAP and Pd/α-Al_2O_3 exhibited

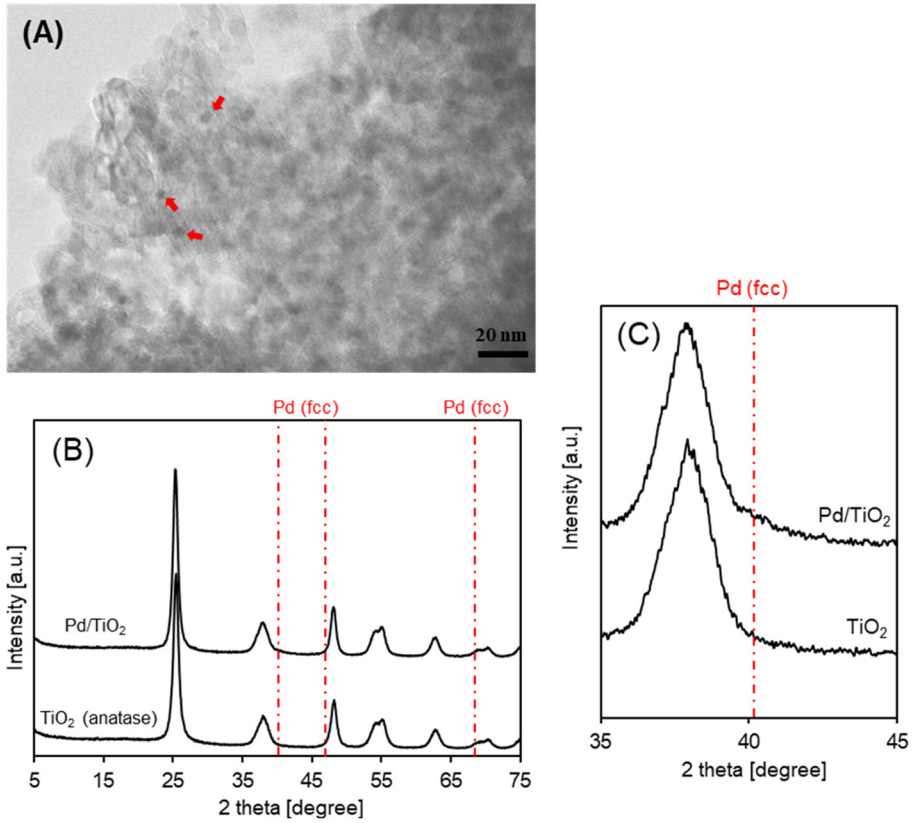

Fig. 4 Characterization data of the Pd/TiO_2 catalyst (Pd = 3 wt%, D = 24%). (A) TEM image, (B) XRD pattern, and (C) XRD pattern around the Pd peak. Conditions: measured after liquid phase reduction at 373 K in water and drying at 383 K in air.

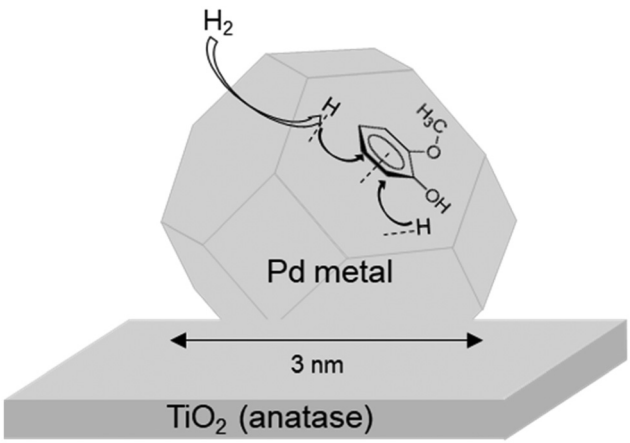

Fig. 5 Plausible active site of the Pd/TiO_2 catalyst for the selective hydrogenation of guaiacol.

comparable selectivity toward 2-MCO to the Pd/TiO_2 catalysts. The contribution of Pd-support interface sites in these two catalysts to side reactions was small: the interface sites had negligible activity (Pd/HAP: much lower activity than Pd/TiO_2) or similar selectivity ($Pd/\alpha\text{-}Al_2O_3$: only slightly lower activity than Pd/TiO_2) to non-interface Pd sites. The Pd/CeO_2 catalyst showed much higher activity while much lower selectivity compared to the Pd/TiO_2 catalysts. This behavior can be explained by the high activity but low selectivity of Pd–CeO_2 interface sites. The good performance of the optimized Pd/TiO_2 catalyst would be due to the small effect of the TiO_2 support on the catalytic performance of Pd-support interfacial sites and appropriate Pd particle size to expose the terrace sites.

3.2. Effect of the reaction conditions

3.2.1. Reaction solvent. The effect of solvent was investigated in the selective hydrogenation of guaiacol over Pd/TiO_2 (Table 2; full selectivity data: Table S9†). The activity (conversion) changed in the order of water > alkanes ≥ no solvent > alcohols ~ THF. Similar solvent effects have also been reported in the hydrogenolysis of guaiacol with Pd/CeO_2.[57] The selectivity was similar between the alkane solutions and no solvent. Then, the reaction test in dodecane solvent was carried out with a large amount of catalyst to compare the selectivity at a similar level of conversion with the reaction operated in water solvent. There was a clear increase in 2-MCol selectivity accompanied by a decrease in 2-MCO selectivity in comparison with the case in the water solvent. Water was thus a better solvent in terms of both activity and selectivity.

To examine the adsorption behavior of the substrate on the catalyst surface in each solvent, the effect of guaiacol concentration on the selective hydrogenation of guaiacol over the Pd/TiO_2 catalyst was investigated at a low conversion level in each

Table 2 Effect of solvents on the selective hydrogenation of guaiacol over the Pd/TiO_2 catalyst

				Yield [C based] (%)				
				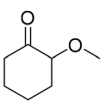	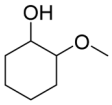	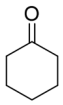		
Entry	Solvent	Amount of catalyst (g)	Conv. (%)	2-MCO	2-MCol		Others	Methanol
1	Water	0.1	40.6	29.6	5.7	2.0	0.7	0.4
2	Methanol	0.1	1.5	0.0	0.1	0.0	0.1	0.0
3	Ethanol	0.1	8.4	4.1	1.2	0.3	0.3	0.1
4	2-Propanol	0.1	1.5	0.4	0.1	0.0	0.2	0.0
5	Tetrahydrofuran	0.1	7.2	3.2	1.8	0.5	1.1	0.2
6	Cyclohexane	0.1	12.7	7.2	3.3	0.8	0.4	0.1
7	Dodecane	0.1	14.9	6.1	2.9	0.4	0.3	0.0
8	Dodecane	0.3	38.0	17.1	15.2	1.4	1.1	0.2
9	No solvent	0.1	13.9	6.9	3.0	0.4	0.4	0.0

Conditions: guaiacol (0.62 g), Pd/TiO_2 (Pd = 3 wt%), solvent (10 g), 373 K, H_2 (1 MPa at r.t.), 4 h.

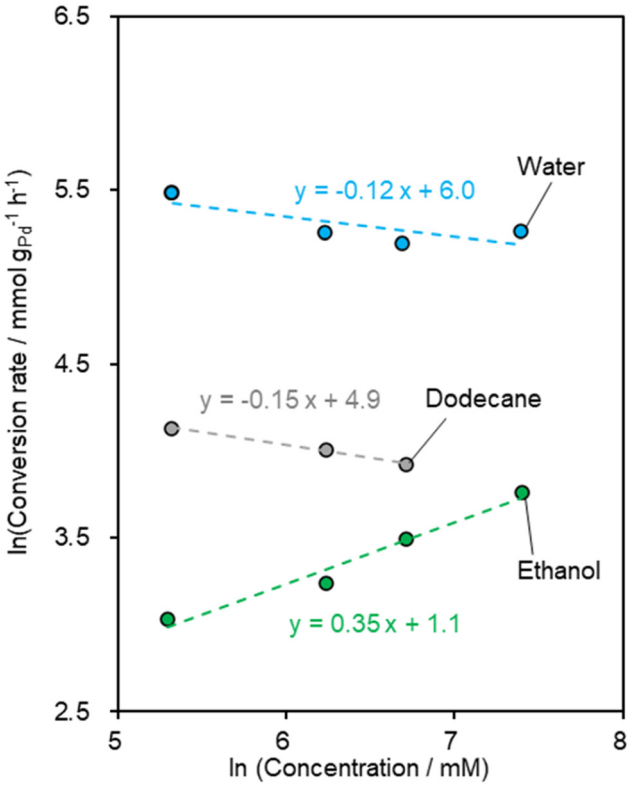

Fig. 6 Double logarithmic plot of the conversion rate as a function of guaiacol concentration for guaiacol hydrogenation over Pd/TiO_2 in various solvents. Conditions: guaiacol (2–16 mmol), Pd/TiO_2 (Pd = 3 wt%, 100 mg), solvent (10 g), H_2 (1 MPa at r.t.), 373 K.

solvent (Fig. 6; detailed data: Table S10† (raw data) and Fig. S2† (conversion–time plot)). The detailed data including the guaiacol conversion rate are shown in Table S10 and Fig. S2.† The reaction order with respect to the guaiacol concentration was *ca.* 0.5 in ethanol and 0 in water and dodecane. These results suggest that the low activity of Pd/TiO_2 in ethanol was due to the competitive adsorption of alcohol and substrate molecules onto the active sites. Meanwhile, the adsorption sites of the Pd/TiO_2 catalyst were fully occupied with guaiacol in the water solvent. For the selective hydrogenation of guaiacol to 2-MCO, the adsorption with the hydrophobic aromatic ring of guaiacol is necessary, and that with the hydrophilic C═O group of 2-MCO decreases the selectivity by promoting over-hydrogenation to 2-MCol.

The effect of solvent was also investigated in the hydrogenation of 2-MCO, which is the most impactful side reaction, over Pd/TiO_2 (entries 10–13, Table S9†). The difference in activity among solvents was smaller in 2-MCO hydrogenation than that in guaiacol hydrogenation. The water solvent accelerates the hydrogenation of guaiacol to 2-MCO but does not accelerate the hydrogenation of 2-MCO to 2-MCol. This behavior can explain the higher selectivity to 2-MCO in water solvent than that in inert solvents, and therefore, the promotion mechanism by water solvent is important for both activity and selectivity in guaiacol hydrogenation to 2-MCO. The promotion ability of water solvent in the guaiacol hydrogenation will be discussed later together with the reaction mechanism.

3.2.2. Reaction temperature. The results of the guaiacol hydrogenation operated at different reaction temperatures (353–393 K) are shown in Fig. 7 (detailed data: Table S11†). The activity increased with the increase of reaction temperature. The selectivity at the low conversion level was similar in this temperature range. However, at the high conversion level, low temperature (353 K) promoted the over-hydrogenation to 2-MCol, and high temperature (393 K) was apt to trigger demethoxylation. A higher 2-MCO yield can be obtained at 373 K, and therefore, we selected 373 K as the standard reaction temperature.

3.2.3. Hydrogen pressure. Table 3 shows the results of the reaction at different hydrogen pressures. Within the H_2 pressure range of 1–5 MPa, the conversion remained almost constant, while the hydrogenation of 2-MCO to 2-MCol pro-

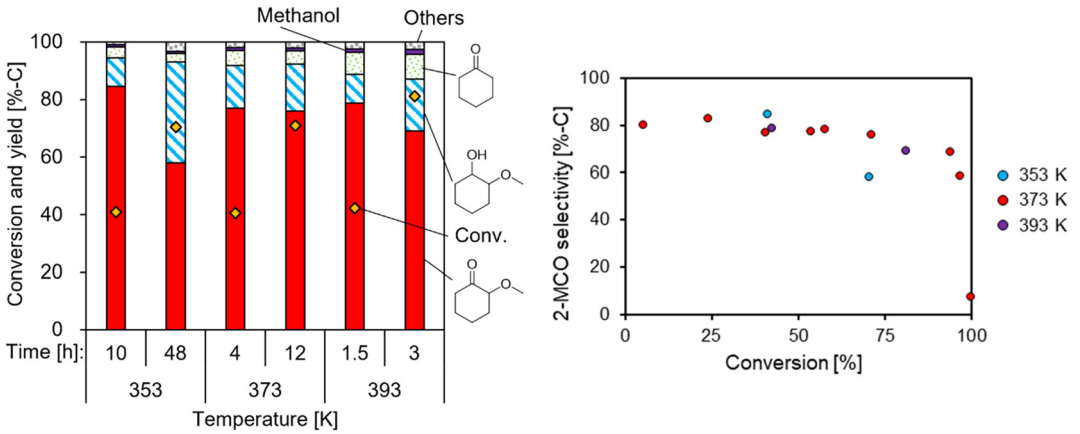

Fig. 7 Effect of reaction temperature and time on the selective hydrogenation of guaiacol over the Pd/TiO_2 catalyst. Conditions: guaiacol (0.62 g), Pd/TiO_2 (Pd = 3 wt%, 100 mg), water (10 g), H_2 (1 MPa at r.t.).

Table 3 Effect of hydrogen pressure on the selective hydrogenation of guaiacol over the Pd/TiO_2 catalyst

				Yield [C based] (%)				
				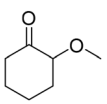	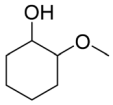	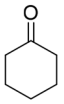		
Entry	H_2 pressure (MPa at r.t.)	Time (h)	Conv. (%)	2-MCO	2-MCol		Others	Methanol
1	0.1	4	21.9	13.9	1.2	1.2	0.3	0.2
2	0.1	6	41.5	27.0	5.1	2.0	0.8	0.4
3	1	4	40.6	29.6	5.7	2.0	0.7	0.4
4	3	4	45.2	28.3	7.9	1.8	0.8	0.3
5	5	4	43.1	26.9	9.8	1.6	0.8	0.3

Conditions: guaiacol (0.62 g), Pd/TiO_2 (Pd = 3 wt%, 100 mg), water (10 g), 373 K.

ceeded slightly faster at higher H_2 pressures. These results indicate the zero-order dependence with respect to hydrogen pressure in the guaiacol hydrogenation within this pressure range, suggesting that the adsorption sites of hydrogen species were fully occupied. The hydrogen pressure of 1 MPa was, therefore, selected as the standard reaction pressure.

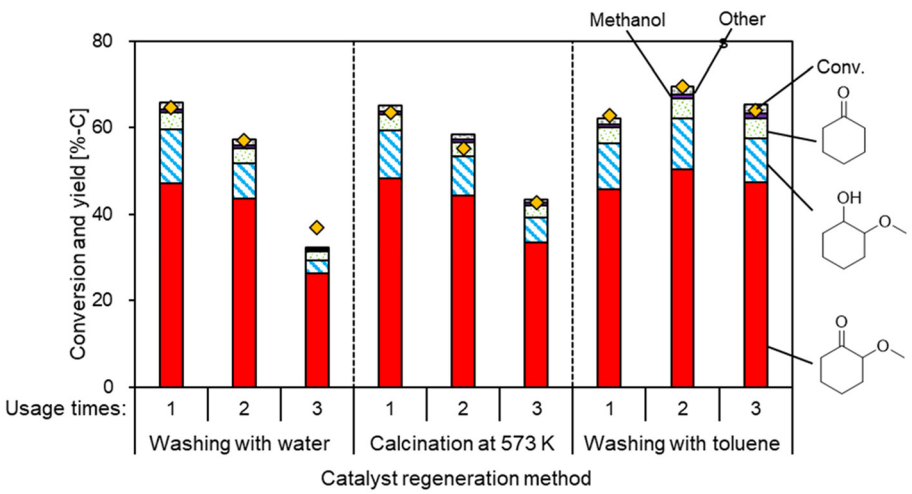

Fig. 8 Reusability of the Pd/TiO_2 catalyst in guaiacol hydrogenation. Conditions: guaiacol (0.62 g), Pd/TiO_2 (Pd = 3 wt%, 200 mg), water (10 g), 373 K, H_2 (1 MPa at r.t.), 4 h.

3.3. Reusability of the Pd/TiO_2 catalyst

The reusability of the Pd/TiO_2 catalyst was evaluated in the selective hydrogenation of guaiacol (Fig. 8; detailed data: Table S12†). The activity of the Pd/TiO_2 catalyst decreased upon its reuse when the recovered catalyst was reused after filtration, washing with water, and drying. The TG-DTA profile for the spent catalyst showed an exothermic weight loss at around 523 K (Fig. S3B†), suggesting that the deposition of organic species on the catalyst surface led to the loss of activity. Thus, the calcination at 573 K as regeneration was then applied to the recovered catalyst after washing with water. Although the activity was partially recovered, the activity of the Pd/TiO_2 catalyst still decreased. The Pd dispersion of the calcined catalysts measured by CO adsorption gradually decreased in the reuses (Table S13†), suggesting that the decrease in the number of active sites due to the agglomeration of Pd particles during the calcination caused the decrease in activity. The increase of Pd particle size was also confirmed in the XRD pattern (Fig. S4†). On the other hand, the washing treatment for the used Pd/TiO_2 catalyst with toluene succeeded in the preservation of catalytic activity. The TG-DTA profile for the catalyst washed with toluene indicated the absence of organic species on the catalyst surface. The organic species dissolved in toluene was analyzed by ^1H NMR spectroscopy (Fig. S5†). Various signals were observed, such as those for alkyl (0.8–1.7 ppm), methoxy (3.0–3.3 ppm; singlet signals), and olefinic (5.5 ppm) protons. Although the possibility of overlapping with toluene signals cannot be ruled out completely, the peaks attributable to aromatic compounds were not detected. These NMR data

Table 4 Substrate scope of the Pd/TiO_2 catalyst

Entry	Substrate	Time [h]	Conv. [%]	Selectivity of each product (C based) [%]			Initial conversion rate [mol h^{-1} g_{Pd}^{-1}]
1	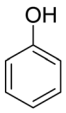	1	99.4	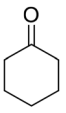 92.0	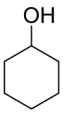 8.0		1.1
2	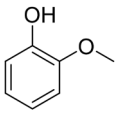	16	93.8	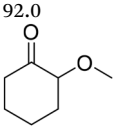 68.5	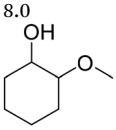 24.1	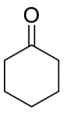 3.9, Others 3.5	0.17
3	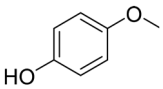	1.5	90.9	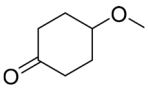 93.7	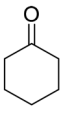 4.0	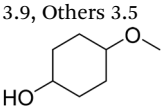 2.3	0.85
4	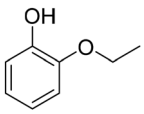	16	92.9	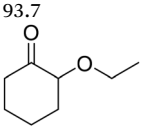 61.7	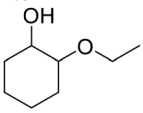 33.2	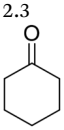 4.7, Others 0.4	0.27
5	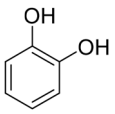	2	94.6	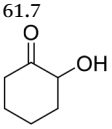 87.7	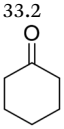 6.8	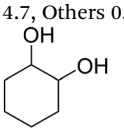 5.5	1.2
6	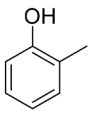	4	93.9	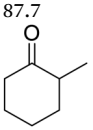 95.1	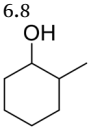 4.9		0.85
7	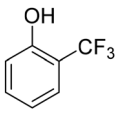	4	96.2	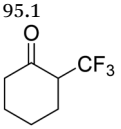 87.6	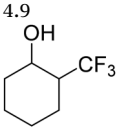 12.4		0.85
8	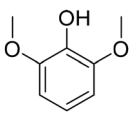	24	28.8	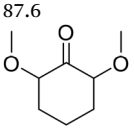 25.0	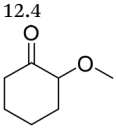 21.9	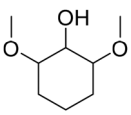 19.2, Others 33.9	0.015

Conditions: substrate (5 mmol), Pd/TiO_2 (Pd = 3 wt%, 100 mg), water (10 g), 373 K, H_2 (1 MPa at r.t.).

indicate that polymeric hydrogenated compounds can be the organic species covering the used catalyst.

3.4. Substrate scope of Pd/TiO_2

The Pd/TiO_2 catalyst was applied to the hydrogenation of various phenolic compounds (Table 4). The detailed data including the time course for each substrate are shown in Table S14.† The hydrogenation of phenol was very fast, and a high yield (92%) of cyclohexanone was obtained. The hydrogenation of 4-methoxyphenol (entry 3) was faster than that of guaiacol (2-methoxyphenol), and demethoxylation from 4-methoxyphenol proceeded more slowly than that from guaiacol. The significantly higher reactivity of 4-methoxyphenol than that of guaiacol has also been reported with other Pd catalysts.[31,55,62] In addition, the effect of substituents at the *ortho* position on the reactivity in the aromatic ring hydrogenation followed the order of $-H \sim -OH > -CH_3 \geq -CF_3 \gg -OCH_3$ (entries 1, 2, and 5–7). This tendency can be mostly explained by steric hindrance due to the size of substituents, while guaiacol is an exception with very low reactivity. The reactivity of 2,6-dimethoxyphenol (syringol) was further lower than guaiacol, and the selectivity to 2,6-dimethoxycyclohexanone was also very low (entry 8). The presence of 2-methoxy groups thus drastically decreased the reactivity. On the other hand, 2-ethoxyphenol showed slightly higher reactivity than guaiacol, although the ethoxy group is bulkier than the methoxy group. The presence of an intramolecular hydrogen bond between the adjacent alkoxy and hydroxy groups is a possible reason for the decrease in reactivity.

We discuss the effect of the methoxy group at the *ortho* position and the reaction mechanism. In the hydrogenation of phenol to cyclohexanone, which is closely related to the selective hydrogenation of guaiacol, two reaction routes have been proposed thus far based on density functional theory (DFT) studies;[60,61,63] (i) direct hydrogenation of adsorbed phenol and (ii) dissociation of adsorbed phenol to adsorbed phenoxide and H followed by hydrogenation. For route (i), the hydrogenation of adsorbed phenol first produces adsorbed dihydrophe-

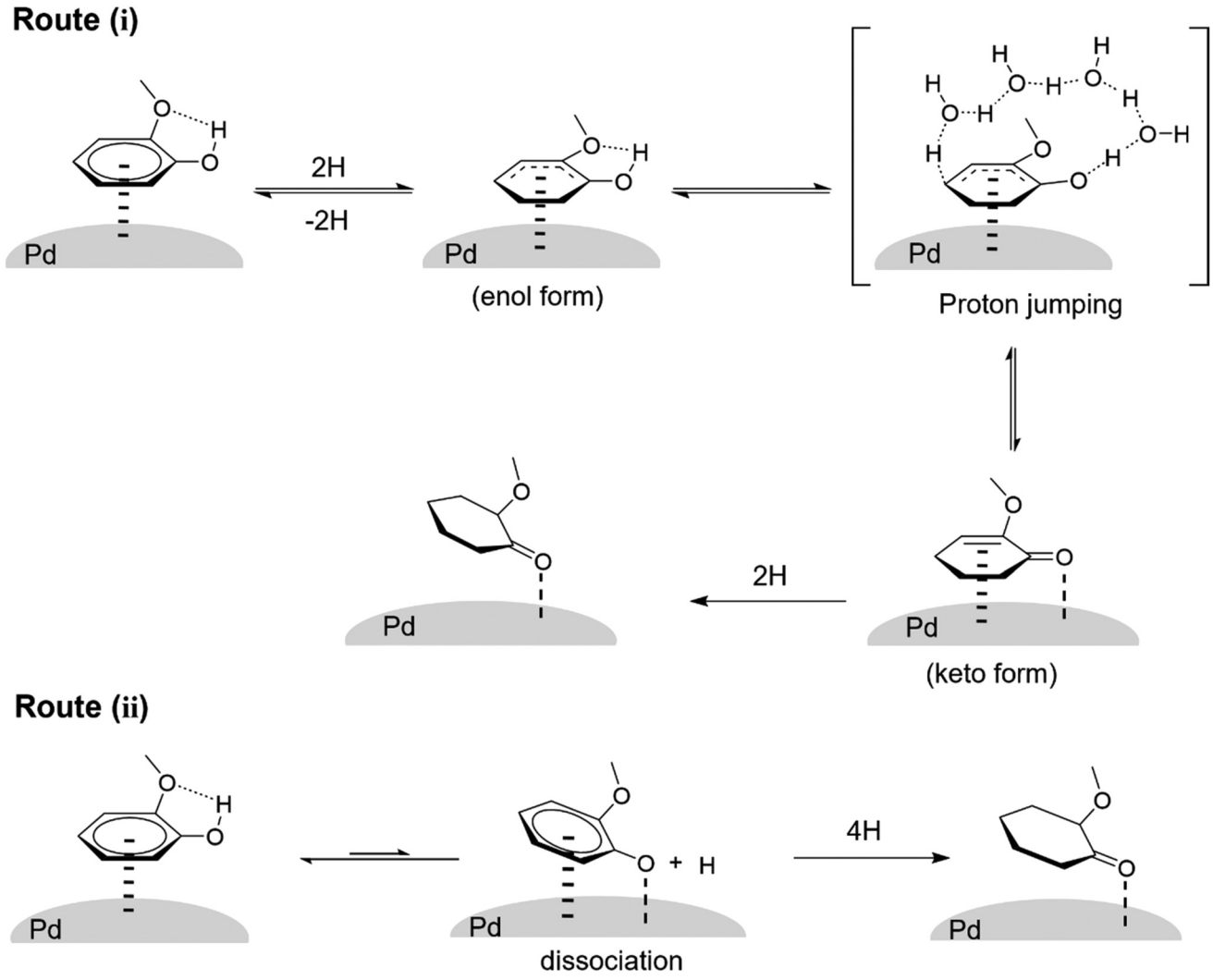

Fig. 9 Possible reaction routes for the selective hydrogenation of guaiacol over the Pd/TiO_2 catalyst in water solvent.

nol. The dihydrophenol is then transformed into cyclohexanone by keto–enol tautomerization, and the cyclohexanone is hydrogenated to cyclohexanone. Lercher *et al.* investigated the effect of water solvent over Pt and Ni catalysts using DFT-based molecular dynamics calculations; the calculated activation energy for keto–enol tautomerization was greatly reduced by the proton transfer *via* proton jumping in solvent molecules compared to the direct proton transfer from oxygen to carbon.[63] The thermodynamic stability of the adsorbed keto form was also found to be enhanced. The positive effect of water solvent observed for guaiacol hydrogenation, but not for 2-MCO hydrogenation, in this study agrees with the calculation report of route (i). Fig. 9 depicts the possible reaction routes for the selective hydrogenation of guaiacol over the Pd/TiO_2 catalyst in a water solvent, and route (i) is the more likely one. The presence of an intramolecular hydrogen bond between the adjacent methoxy and hydroxy groups in guaiacol may suppress the dissociation of the O–H bond and the reaction route (ii). The reaction route (i) is also slowed down by the presence of the 2-methoxy group because of the stabilization of the enol form. Still, the water solvent promotes the keto–enol formation, and 2-MCO is produced in this route.

The formation ratios of *cis*/*trans* isomers of 2-MCol from guaiacol and 2-MCO as substrates were compared (Table S15†). From 2-MCO, the *cis* : *trans* ratio of 2-MCol was almost 1 : 1 regardless of the reaction time. On the other hand, the *cis* : *trans* ratio was about 2 : 1 from guaiacol when the overreaction of 2-MCO was minor. When the produced 2-MCO was almost completely converted to 2-MCol (24 h), the *cis* : *trans* ratio became about 1.5 : 1. These data indicated that part of 2-MCol was directly produced from guaiacol by the *syn* addition of hydrogen species to the unsaturated ring adsorbed on the metal surfaces. The large contribution of the direct total hydrogenation of guaiacol can be more reasonably explained by route (i) in Fig. 9. The enol form of adsorbed dihydroguaiacol is more stabilized by the hydrogen bond than the cases of other phenolic compounds, and the further hydrogenation of the adsorbed enol form, which can be regarded as the direct hydrogenation of guaiacol, becomes easier. These results and considerations further support the aforementioned possibility of route (i) as the more plausible route than route (ii).

The performance of the Pd/TiO_2 catalyst is compared with that of other catalysts in previous reports (Table S1†). For the hydrogenation of phenolic compounds without methoxy groups such as *o*-cresol (2-methylphenol) and catechol (2-hydroxyphenol), the Pd/TiO_2 catalyst exhibited slightly lower selectivity towards the target ketones than the reported best catalysts with sophisticated supports because of the over-hydrogenation. In contrast, in the selective hydrogenation of phenol derivatives containing methoxy groups, the Pd/TiO_2 catalyst performed comparable to or even better than other catalysts. A difference from reported catalysts is the lower activity of the Pd/TiO_2 catalyst for demethoxylation. Many reported catalysts used basic supports to offer adsorption sites for the weakly acidic phenolic group to promote phenol hydrogenation over cyclohexanone hydrogenation; however, basic sites also promote demethoxylation during the hydrogenation of methoxyphenols to decrease the selectivity to methoxycyclohexanones.[47,48,51]

4. Conclusions

We have reported the hydrogenation of guaiacol to 2-methoxycyclohexanone in good yields (up to 65%) using the Pd/TiO_2 catalyst in an aqueous solution. The chloride ion promotes the demethoxylation of guaiacol to decrease the selectivity, and thus the use of a Cl-free precursor is preferred. In reusable tests, the recovered catalyst after washing with water or calcination exhibited lower activity than the fresh catalyst; in stark contrast, the catalyst could be reused by washing with toluene. Furthermore, the catalyst was applicable to the selective hydrogenation of various phenolic compounds and produced the corresponding ketones in high yields. In particular, the Pd/TiO_2 catalyst is good at the selective hydrogenation of methoxyphenols in comparison with reported catalysts using a Pd + basic support. Through the characterization of Pd dispersion by CO adsorption, we determined the optimal Pd particle size for the formation of 2-MCO from guaiacol to be approximately 3 nm because of the balance of good dispersion and exposure to flat metal surfaces. Considering the solvent effect and *cis*/*trans* formation ratio of 2-methoxycyclohexanol, the reaction route involving keto–enol tautomerization of intermediates is more plausible.

Data availability

The data supporting this article have been included as part of the ESI.†

Conflicts of interest

There are no conflicts to declare.

Acknowledgements

This work was supported by JSPS KAKENHI grants 23H05404, 23K20034, and 23K26451. The authors also appreciate the assistance provided by the Technical Division, School of Engineering, Tohoku University, in STEM measurement.

References

1 A. Corma, S. Iborra and A. Velty, *Chem. Rev.*, 2007, **107**, 2411–2502.
2 M. Besson, P. Gallezot and C. Pinel, *Chem. Rev.*, 2014, **114**, 1827–1870.
3 B. M. Stadler, C. Wulf, T. Werner, S. Tin and J. G. Vries, *ACS Catal.*, 2019, **9**, 8012–8067.

4 D. M. Alonso, J. Q. Bond and J. A. Dumesic, *Green Chem.*, 2010, **12**, 1493–1513.
5 G. W. Huber, S. Iborra and A. Corma, *Chem. Rev.*, 2006, **106**, 4044–4098.
6 H. Wang, J. Male and Y. Wang, *ACS Catal.*, 2013, **3**, 1047–1070.
7 Q. Lu, X. Jiang, Z. Zhang, X. Zhang, G. Song, H. Wang, Y. Yuan and Y. Chang, *Green Chem.*, 2021, **23**, 9348–9376.
8 J. Yang, S. Luan, M. Dong, Y. Wu, X. Xing, X. Liu, J. Xiang, Z. Zhao, S. Li, B. Zhang, H. Liu and B. Han, *CCS Chem.*, 2024, **6**, 709–718.
9 B. Zhang, Q. Meng, H. Liu and B. Han, *Acc. Chem. Res.*, 2023, **56**, 3558–3571.
10 K. Yamazaki, A. Segawa, H. Mazaki, N. Hiyoshi, N. Mimura, O. Sato and A. Yamaguchi, *RSC Adv.*, 2023, **13**, 13472–13476.
11 B. Liu, M. Sanchez, J. Truong, P. C. Ford and M. M. Abu-Omar, *Green Chem.*, 2022, **24**, 4958–4968.
12 D. J. Nowakowski, A. V. Bridgwater, D. C. Elliott, D. Meier and P. Wild, *J. Anal. Appl. Pyrolysis*, 2010, **88**, 53–72.
13 T. S. Nguyen, D. Laurenti, P. Afanasiev, Z. Konuspayeva and L. Piccolo, *J. Catal.*, 2016, **344**, 136–140.
14 J. Mao, J. Zhou, Z. Xia, Z. Wang, Z. Xu, W. Xu, P. Yan, K. Liu, X. Guo and Z. C. Zhang, *ACS Catal.*, 2017, **7**, 695–705.
15 X. Jin, B. Yin, Q. Xia, T. Fang, J. Shen, L. Kuang and C. Yang, *ChemSusChem*, 2018, **12**, 71–92.
16 A. Gutierrez, R. K. Kaika, M. L. Honkela, R. Slioor and A. O. I. Krause, *Catal. Today*, 2009, **147**, 239–246.
17 M. V. Bykova, D. Y. Ermakov, V. V. Kaichev, O. A. Bulavchenko, A. A. Saraev, M. Y. Lebedev and V. A. Yakovlev, *Appl. Catal., B*, 2012, **113**, 296–307.
18 R. N. Olcese, M. Bettahar, D. Petitjean, B. Malaman, F. Giovanella and A. Dufour, *Appl. Catal., B*, 2012, **115**, 63–73.
19 Y. C. Lin, C. L. Li, H. P. Wan, H. T. Lee and C. F. Liu, *Energy Fuels*, 2011, **25**, 890–896.
20 K. Zhang, Q. Meng, H. Wu, J. Yan, X. Mei, P. An, L. Zheng, J. Zhang, M. He and B. Han, *J. Am. Chem. Soc.*, 2022, **144**, 20834–20846.
21 M. M. Ambursa, J. C. Juan, Y. Yahaya, Y. H. T. Yap, Y. C. Lin and H. V. Lee, *Renewable Sustainable Energy Rev.*, 2021, **138**, 110667.
22 V. S. Prabhudesai, L. Gurrala and R. Vinu, *Energy Fuels*, 2022, **36**, 1155–1188.
23 X. Wang, M. Arai, Q. Wu, C. Zhang and F. Zhao, *Green Chem.*, 2020, **22**, 8140–8168.
24 A. Yamaguchi, Y. Murakami, K. Yamazaki, M. Shirai and N. Hiyoshi, *Catal. Today*, 2024, **425**, 114356.
25H. Yang, X. Zhu, H. W. Amini, B. Fachri, M. Ahmadi, G. H. Brink, P. J. Deuss and H. J. Heeres, *Appl. Catal., A*, 2023, **654**, 119062.
26 R. Beerthuis, G. Rothenberg and N. R. Shiju, *Green Chem.*, 2015, **17**, 1341–1361.
27 J. Rios, J. Lebeau, T. Yang, S. Li and M. D. Lynch, *Green Chem.*, 2021, **23**, 3172–3190.
28 Y. Nakagawa, M. Yabushita and K. Tomishige, *Asian J. Org. Chem.*, 2023, **12**, e202300409.
29 J. Rios, J. Lebeau, T. Yang, S. Li and M. D. Lynch, *Green Chem.*, 2021, **23**, 3172–3190.
30 K. Hatakeyama, Y. Nakagawa, M. Tamura and K. Tomishige, *Green Chem.*, 2020, **22**, 4962–4974.
31 G. Xu, J. Guo, Y. Zhang, Y. Fu, J. Chen, L. Ma and Q. Guo, *ChemCatChem*, 2015, **7**, 2485–2492.
32 H. Chen and J. Sun, *J. Ind. Eng. Chem.*, 2021, **94**, 78–91.
33 Y. Liao, S. Koekewijn, G. V. Bossche, J. V. Aelst, S. V. D. Bosch, T. Renders, K. Navare, T. Nicokai, K. V. Aelst, M. Maesen, H. Matsusima, J. M. Thevelein, K. V. Acker, B. Lagrain, D. Verboekend and B. F. Sels, *Science*, 2020, **367**, 1385.
34 H. Wang, W. Wang, R. Wang, X. Jiang, W. Li, Z. H. He, K. Wang, Y. Yang, Q. Li and Z. T. Liu, *Appl. Catal., A*, 2024, **670**, 119520.
35 J. Zhang, H. Zhao, L. Yang, H. Jiang, Y. Du and R. Chen, *Appl. Catal., A*, 2023, **666**, 119428.
36 Z. Wang, B. Ye, R. Zhou, Z. Zhong, P. Chen and Z. Hou, *Appl. Catal., A*, 2023, **657**, 119144.
37 D. Yin, R. Ji, J. Zhang, S. Yu, L. Li, S. Liu, L. Jiang, Z. Song and Y. Liu, *Fuel*, 2023, **333**, 126481.
38 D. Yin, R. Ji, F. Lv, L. Jiang, J. Zhang, M. Liu, Z. Jia, S. Yu, R. Zhao and Y. Liu, *Fuel*, 2023, **332**, 126060.
39 X. Zhu, J. Zhang, H. Jiang and R. Chen, *Appl. Catal., A*, 2022, **634**, 118538.
40 C. Yang, K. Li, J. Wang and S. Zhou, *Appl. Catal., A*, 2021, **610**, 117961.
41 Y. Wang, J. Yao, H. Li, D. Su and M. Antonietti, *J. Am. Chem. Soc.*, 2011, **133**, 2362–2365.
42 Y. Shao, J. Zhang, H. Jiang and R. Chen, *Ind. Eng. Chem. Res.*, 2021, **60**, 5806–5815.
43 H. Li, T. She, G. Chen, M. Sun, L. Niu and G. Bai, *Mol. Catal.*, 2021, **504**, 111493.
44 S. Xu, J. Du, Q. Zhou, H. Li, C. Wang and J. Tang, *Colloid Interface Sci.*, 2021, **604**, 876–884.
45 M. Aliahmadi, M. Davoudi and A. N. Kharat, *React. Kinet., Mech. Catal.*, 2020, **131**, 819–828.
46 J. Zhang, C. Zhang, H. Jiang, Y. Liu and R. Chen, *Ind. Eng. Chem. Res.*, 2020, **59**, 10768–10777.
47 M. Ishikawa, M. Tamura, Y. Nakagawa and K. Tomishige, *Appl. Catal., B*, 2016, **182**, 193–203.
48 Y. Nakagawa, M. Ishikawa, M. Tamura and K. Tomishige, *Green Chem.*, 2014, **16**, 2197–2203.
49 C. Li, Y. Nakagawa, M. Tamura, A. Nakayama and K. Tomishige, *ACS Catal.*, 2020, **10**, 14624–14639.
50 C. R. Lee, J. S. Yoon, Y. W. Suh, J. W. Choi, J. M. Ha, D. J. Suh and Y. K. Park, *Catal. Commun.*, 2012, **17**, 54–58.
51 L. Huang, F. Tang, P. Liu, W. Xiong, S. Jia, F. Hao, Y. Lv and H. Luo, *Fuel*, 2022, **327**, 125115.
52 S. Wang, L. Yang, T. Zhu, N. Jiang, F. Li, H. Wang, C. Zhang and H. Song, *React. Chem. Eng.*, 2022, **7**, 170–180.
53 F. Zhang, C. Wu, S. Wang, S. Wang, T. Li, L. Zou, H. Yu and H. Yin, *Catal. Sci. Technol.*, 2022, **12**, 2257–2264.
54 P. Yan, P. Tian, K. Li, M. A. C. Stuart, J. Wang, X. Yu and S. Zhou, *Chem. Eng. J.*, 2020, **397**, 125484.

55 H. Zhang, A. Han, K. Okumura, L. Zhong, S. Li, S. Jaenicke and G. K. Chuah, *J. Catal.*, 2018, **364**, 354–365.
56 A. Chen, G. Zhao, J. Chen, L. Chen and Y. Yu, *RSC Adv.*, 2013, **3**, 4171–4175.
57 H. Zhou, H. Wang, A. D. Sadow and I. I. Slowing, *Appl. Catal., B*, 2020, **270**, 118890.
58 L. L. Sheu, Z. Karpinski and W. M. H. Sachtler, *J. Phys. Chem.*, 1989, **93**, 4890–4894.
59 G. Bergeret and P. Gallezot, Particle Size and Dispersion Measurements, in *Handbook of Heterogeneous Catalysis*, ed. G. Ertl, H. Knözinger, F. Schüth and J. Weitkamp, Wiley-VCH, Weinheim, 2008, pp. 738–765.
60 G. Li, J. Han, H. Wang, H. Zhu and Q. Ge, *ACS Catal.*, 2015, **5**, 2009–2016.
61 H. Zhou, B. Han, T. Liu, X. Zhong, G. Zhuang and J. Wang, *Green Chem.*, 2017, **19**, 3585–3594.
62 S. Fehn, M. Zaheer, C. E. Denner, M. Friedrich and R. Kempe, *New J. Chem.*, 2016, **40**, 9252–9256.
63 Y. Yoon, R. Rousseau, R. S. Weber, D. Mei and J. A. Lercher, *J. Am. Chem. Soc.*, 2014, **136**, 10287–10298.